A Stochastic-Dynamic-Optimization Approach to Estimating the Capacity Value of Energy Storage

Hyeong Jun Kim, *Student Member, IEEE,* Ramteen Sioshansi, *Fellow, IEEE,*
Eamonn Lannoye, *Senior Member, IEEE,* and Erik Ela, *Senior Member, IEEE*

***Abstract*—Energy storage can contribute to the resource-adequacy needs of power systems. However, the energy-limited nature of energy storage complicates estimating its resource-adequacy contribution. Energy storage that discharges to mitigate a loss-of-load event may have less energy available to mitigate a subsequent loss-of-load event. We present a stochastic-dynamic-optimization approach to capture such impacts endogenously. We demonstrate our approach using an example and two case studies, which show that energy storage's capacity value is sensitive to the load patterns of the system in which it is deployed.**

***Index Terms*—Power system security and risk analysis, capacity value, reliability theory, dynamic programming, energy storage**

NOMENCLATURE

Indices, Sets, and Parameters

$\mathcal{A}_t(l_t,\omega_t)$	hour-t decisions that are feasible if the system state is (l_t,ω_t)
e	loss-of-load expectation (LOLE)
$e^{\bar{M}}$	LOLE with $\bar{M}$ MW of load added during each hour
G_t	hour-t generating capacity available (MW)
$\bar{h}$	energy-carrying capacity of energy storage (h)
$\mathcal{I}_{t+1}(y)$	hour-t states from which an optimal policy results in the hour-$(t+1)$ state of energy (SOE) of energy storage being y
$\bar{l}_1$	hour-1 starting SOE of energy storage (MWh)
$\bar{M}$	hourly load that is added in computation of effective load-carrying capability (MW)
M_t	hour-t load (MW)
p_t	hour-t loss-of-load probability
$\bar{R}$	power capacity of energy storage (MW)
t	time index
T	number of time periods in model horizon
$\bar{V}$	penalty imposed on energy storage for a power-output shortfall ($/MW)
Δ	set of decision policies
η	round-trip efficiency of energy storage (p.u.)
$\xi_t(y)$	probability that the hour-t SOE of energy storage is y
π_t	hour-t energy price ($/MWh)

State Variables

l_t	beginning hour-t SOE of energy storage (MWh)
ω_t	equals 0 if the system has a capacity shortfall during hour t and equals 1 otherwise

Decision Variables

c_t	hour-t charging into energy storage (MW)
d_t	hour-t discharging from energy storage (MW)

Decision Policies

δ	a decision policy
$c_t^\delta(l_t,\omega_t)$	hour-t charging policy (MW)
$d_t^\delta(l_t,\omega_t)$	hour-t discharging policy (MW)

Manuscript received 21 November, 2020; revised 4 May, 2021, 29 June, 2021, and 1 September, 2021; accepted 2 September, 2021. This work was supported by National Science Foundation grant 1808169 and Electric Power Research Institute grant 00-10007617. *(Corresponding author: Hyeong Jun Kim.)*

H. J. Kim is with Department of Integrated Systems Engineering, The Ohio State University, Columbus, OH 43210-1271, USA (e-mail: kim.5206@buckeyemail.osu.edu.

R. Sioshansi is with Department of Integrated Systems Engineering and Department of Electrical and Computer Engineering, The Ohio State University, Columbus, OH 43210-1271, USA (e-mail: sioshansi.1@osu.edu).

E. Lannoye is with Grid Operations & Planning, EPRI Europe, Dublin, Ireland (elannoye@epri.com).

E. Ela is with Power Delivery and Utilization Department, Electric Power Research Institute, Palo Alto, CA 94304-1395, USA (e-mail: eela@epri.com).

I. INTRODUCTION

ENERGY storage can be used for numerous services, including energy shifting, ancillary services, resource adequacy, investment deferral, and end-user applications [1]. Given its capital costs, the owner may use an energy-storage asset for multiple applications [2], [3]. Its energy-limited nature makes using energy storage for resource adequacy challenging, however. For instance, if energy storage discharges during hour t to earn energy revenue or to alleviate a loss-of-load event, its state of energy (SOE) and ability to alleviate a subsequent loss-of-load event may be reduced. Given these complications, operators of restructured markets are seeking methods to ascribe capacity value to energy-storage resources.

The literature takes a number of approaches to estimating the resource-adequacy contribution of energy storage. One approach uses approximations, *e.g.*, based on capacity factors [4], [5] or load-duration-curve analyses [6]. Such methods can be computationally efficient but limited, insomuch as they rely on having known load or energy-storage-operation profiles.

Another approach to estimating the resource-adequacy contribution of energy storage employs Monte Carlo methods [7]. Bagen and Billinton [8] use such methodology in examining the impact of energy storage on expected unserved energy. Hu *et al*. [9] employ a similar approach and consider different energy-storage-dispatch strategies. Koh *et al*. [10] develop a

hybrid method that combines sequential energy-storage simulation with convolution of the load-duration curve and solar-generation pattern. Zhou *et al*. [11] use a sequential model to compute the effective load-carrying capability (ELCC) of energy storage that is used for load shaving. Konstantelos *et al*. [12] and Konstantelos and Strbac [13] study the impact of network topology and reliability on the ELCC of energy storage. A chief disadvantage of Monte Carlo techniques is their computational expense.

A third body of work applies analytic methods to estimating the resource-adequacy contribution of energy storage [14]. A key challenge of such methods is the need to represent energy-storage operations and chronology. As such, many analytic techniques rely on strong assumptions to maintain tractability. Klöckl and Papaefthymiou [15] develop an approach for expressing the SOE of energy storage as a function of its initial SOE and load. For simplicity, their approach assumes that energy storage has unlimited energy-carrying capacity. Edwards *et al*. [16] employ non-sequential simulation, assuming that energy storage always can be charged fully overnight. Sioshansi *et al*. [17] develop an energy-storage-operation model that assumes that energy storage is operated to maximize arbitrage value without anticipating potential future loss-of-load events in making operational decisions.

The aim of this paper is to expand upon these analytic methods, and the work of Sioshansi *et al*. [17] in particular, by relaxing the assumption of myopic energy-storage operations. We propose a stochastic-dynamic-optimization model that determines the operation of energy storage accounting for energy prices and potential loss-of-load events. Loss-of-load events are important to the energy storage, because we assume that it participates in a capacity market with non-performance penalties (*e.g*., ISO New England's Forward Capacity Market). We develop a technique that uses optimal decision policies to estimate the resource-adequacy contribution of energy storage. We demonstrate our proposed methodology using two case studies, which are based on summer- and winter-peaking systems. Because the case-study data are proprietary, we include also a simple example, the complete underlying data of which we provide. Using our example and case studies, we show how load patterns impact the resource-adequacy contribution of energy storage. We show also that myopic decision making can reduce the capacity value of energy storage, as its SOE may be exhausted during periods with high loss-of-load probabilities (LOLPs) that follow a high-price period.

Thus, this paper has two primary contributions to the extant literature that build upon the work of Sioshansi *et al*. [17]. First, our proposed methodology provides more robust estimates of the resource-adequacy contribution of energy storage than methods in the existing literature. This is because our methodology accounts for uncertainty (*e.g*., loss-of-load events) explicitly in making operational decisions. Sioshansi *et al*. [17] use a deterministic modeling approach. Second, our optimization model can be used to co-optimize the use of energy storage for providing energy-shifting and resource-adequacy services simultaneously. Our example and case studies demonstrate the impact that non-performance penalties have on the operation of energy storage, how the model trades-off between the two services, and the resultant impact on the resource-adequacy contribution of energy storage. Indeed, by contrasting results with and without non-performance penalties, we demonstrate our proposed model improving over the previous work of Sioshansi *et al*. [17].

The remainder of this paper is organized as follows. Section II details our proposed methodology. Section III illustrates our methodology with a simple example. Sections IV and V summarize, respectively, the data that underlie and the results of two comprehensive case studies, to which we apply our proposed methodology. Section VI concludes.

II. Modeling Approach

Our approach to estimating the capacity value of energy storage consists of four major steps, which are detailed in the following subsections. For ease of exposition, we assume throughout that everything is modeled at hourly time steps over a year-long horizon. There is no loss of generality in these assumptions.

Our first modeling step determines the reliability of the base system (*i.e*., without the energy storage), which we measure using hourly LOLPs. LOLPs are needed for our second step, which determines the operation of the energy storage with a stochastic-dynamic-optimization model. Another reliability metric could be used alongside LOLPs for measuring system reliability, however. The third step uses the optimized decision policies to determine the probability distributions of the SOE of energy storage during each hour. The final step uses these probability distributions to determine the resource-adequacy contribution of energy storage. We measure this contribution using ELCC [18], [19], but other metrics could be used.

A. Reliability Modeling of Base System

The hour-t LOLP is defined as:

$$p_t = \text{Prob}\left\{G_t < M_t\right\}, \tag{1}$$

where $\text{Prob}\left\{\cdot\right\}$ represents any randomness that impacts the ability of the system to serve load [14]. As is common of modeling power-system reliability, generators are assumed to be available to produce power at nameplate capacity, so long as they are not suffering an outage or failure that prevents their operation. LOLE is defined as:

$$e = \sum_{t=1}^{T} p_t.$$

B. Energy-Storage-Operation Model

We formulate a stochastic-dynamic-optimization problem to determine the operation of energy storage. The primary source of uncertainty is loss-of-load events, the probabilities of which are given by the LOLPs that are given by (1). Thus, our model assumes that the energy-storage owner knows the likelihood of future loss-of-load events. Other uncertainties (*e.g*., energy prices) could be modeled as well. The model maximizes expected revenues from energy shifting, less any penalties that are assessed against energy storage for having a

power-output shortfall during a loss-of-load event. We provide an explicit model formulation, by detailing the stages, state and decision variables, state-transition and objective-contribution functions, and constraints [20], [21].

1) Stages: Each hour, $t = 1, \ldots, T$, is a stage.

2) State Variables: $\forall t = 1, \ldots, T$, ω_t is an exogenous random state variable that indicates whether the system experiences an hour-t capacity shortfall. $\forall t = 1, \ldots, T$, l_t are endogenous state variables.

3) Decision Variables: $\forall t = 1, \ldots, T$, c_t and d_t are decision variables.

4) State-Transition Functions: $\{\omega_t\}_{t=1}^{T}$ are determined exogenously and randomly. We have that $\forall t = 1, \ldots, T$, ω_t equals 0 and 1 with probabilities p_t and $1 - p_t$, respectively. $\{l_t\}_{t=1}^{T}$ evolve endogenously according to:

$$l_{t+1} = l_t + c_t - d_t; \forall t = 1, \ldots, T; \tag{2}$$

where:

$$l_1 = \bar{l}_1. \tag{3}$$

Equation (2) does not account explicitly for energy that is lost during the energy-storage cycle. Instead, efficiency losses are captured in the objective. For instance, if $\eta = 0.75$, then for each MW that is charged into the energy storage during the full duration of hour t, l_{t+1} increases by 1 MWh. Each MW of stored energy that is discharged during a full hour reduces the SOE of energy storage by 1 MWh, but outputs only 0.75 MWh to be provided to the power system (*e.g.*, to earn energy revenue or to alleviate a loss-of-load event). We model energy losses in this way so the model has a finite state space, which allows for solving the model efficiently using backward recursion [17], [20], [21]. The assumption of different charging and discharging rates is realistic, as modern energy-storage technologies can be designed easily with different charging and discharging capacities [22], [23].

5) Constraints: Charging and discharging are limited by the power capacity of the energy storage:

$$0 \leq c_t \leq \bar{R} \cdot \omega_t; \forall t = 1, \ldots, T; \tag{4}$$

$$0 \leq d_t \leq \bar{R}; \forall t = 1, \ldots, T. \tag{5}$$

Moreover, (4) does not allow the energy storage to charge during a loss-of-load event, as doing so would exacerbate the capacity shortfall and involuntary load curtailment.

The energy storage has SOE limits:

$$0 \leq l_{t+1} \leq \bar{h} \cdot \bar{R}; \forall t = 1, \ldots, T; \tag{6}$$

as well. Strictly speaking, these are not valid constraints, because they restrict the state variable, l_{t+1}, whereas constraints should restrict decision variables [20], [21]. We can convert these to the valid constraints:

$$-l_t \leq c_t - d_t \leq \bar{h} \cdot \bar{R} - l_t; \forall t = 1, \ldots, T; \tag{7}$$

by substituting (2) into (6).

We define $\mathcal{A}_t(l_t, \omega_t) = \{c_t, d_t | (4), (5), \text{and } (7)\}$, $\forall t = 1, \ldots, T$, as stage-t decisions that are feasible if the stage-t state is (l_t, ω_t).

6) Objective-Contribution Functions: The hour-t objective-contribution function is:

$$K_t(c_t, d_t; l_t, \omega_t) = \pi_t \cdot (\eta d_t - c_t) - (1 - \omega_t)\bar{V}\eta \cdot (\bar{R} - d_t); \tag{8}$$

$\forall t = 1, \ldots, T$. This function consists of two terms. The first gives the net operating revenue that is earned from energy shifting. As noted in Section II-B4, we account for the energy that is lost in the energy-storage cycle by applying η to discharged energy in (8). Alternatively, one could apply the energy losses in (2). We apply energy losses in (8) because doing so gives us a finite state space, which eases solution of the dynamic optimization model and computation of the distributions of the SOE of energy storage during each hour [17], [20], [21].

The second term in (8) represents the penalty that is levied on the energy storage for not discharging up to its power capacity if a loss-of-load event occurs. This term is meant to mimic the function of non-performance penalties that some markets impose on capacity resources. For instance, PJM Interconnection's Reliability Pricing Model imposes non-performance penalties on resources that clear the capacity auction [24]. ISO New England's Forward Capacity Market does the same.[1]

If there is not an hour-t loss-of-load event, the penalty term in (8) vanishes and does not impact energy-storage operations. On the other hand, if there is a loss-of-load event, the second term in (8) remains and penalizes the energy storage for not discharging at full power. Thus, if in the absence of an hour-t loss-of-load event, energy storage would discharge during hour t, it is optimal for it to do so during hour t in the presence of a loss-of-load event.

7) Complete Optimization Model and Optimal Decision Policies: To give the complete model, we define Δ as the set of feasible policies. $\forall t = 1, \ldots, T$, a policy, $A_t^{\delta}(l_t, \omega_t)$, is a mapping between stage-t state, (l_t, ω_t), and a feasible set of stage-t decisions, $(c_t, d_t) \in \mathcal{A}_t(l_t, \omega_t)$. $\forall \delta \in \Delta$ we define:

$$G_t^{\delta}(l_t, \omega_t) = \mathbb{E}\left[\sum_{\tau=t}^{T} K_\tau\left(A_\tau^{\delta}(l_\tau, \omega_\tau); l_\tau, \omega_\tau\right) \middle| \omega_t\right]; \quad \forall t = 1, \ldots, T; \tag{9}$$

as the total net operating profit from stage t onward. Equation (9) includes an expected-value operator, because of uncertainty. We focus our analysis on loss-of-load events as being the primary source of uncertainty. However, other factors (*e.g.*, energy prices) could be modeled as uncertain as well. The objective is to find an optimal policy, δ^*, that satisfies:

$$G_t^{\delta^*}(l_t, \omega_t) = \sup_{\delta \in \Delta} G_t^{\delta}(l_t, \omega_t); \forall t = 1, \ldots, T.$$

Our model is solved using backward recursion [20], [21], which can be applied efficiently because the model has finite optimal action and state spaces [17]. These finite optimal action and state spaces arise from the way in which we model energy losses that are associated with cycling energy through the energy storage. Employing dynamic optimization and

[1] *cf.* Federal Energy Regulatory Commission docket number ER21-1010-000.

backward recursion simplifies our overall proposed methodology, because backward recursion yields decision policies. These decision policies specify an optimal stage-t action for *any* possible stage-t state, not only the state that results from an optimal sequence of decisions. Decision policies allow us to determine efficiently how the SOE and operation of energy storage evolve after random loss-of-load events occur, which change the system state. Energy-storage operations could be optimized using other techniques (*e.g.*, linear or mixed-integer optimization). However, such models would need to be solved repeatedly in an online manner to 'construct' decision-policy information.

Hereafter we let $\{c_t^{\delta^*}(l_t,\omega_t)\}_{t=1}^T$ and $\{d_t^{\delta^*}(l_t,\omega_t)\}_{t=1}^T$ represent optimal charging and discharging decision policies, where by definition we have:

$$A_t^{\delta^*}(l_t,\omega_t) = \left(c_t^{\delta^*}(l_t,\omega_t), d_t^{\delta^*}(l_t,\omega_t)\right); \forall t = 1,\ldots,T.$$

C. Probability Distribution of l_t

$\{l_t\}_{t=1}^T$ are random because δ^* depends on $\{\omega_\tau\}_{\tau=1}^t$. We can compute the probability distribution of $\{l_t\}_{t=1}^T$ using δ^* and $\{p_t\}_{t=1}^T$. To do so, we define, $\forall t = 1,\ldots,T-1$:

$$\mathcal{I}_{t+1}(y) = \left\{ l_t,\omega_t \,\middle|\, l_t + c_t^{\delta^*}(l_t,\omega_t) - d_t^{\delta^*}(l_t,\omega_t) = y \right\};$$

as the set of stage-t system states, (l_t,ω_t), from which δ^* results in the stage-$(t+1)$ SOE of energy storage being y. As discussed in Section II-B7, $\forall t = 1,\ldots,T-1$, $\mathcal{I}_{t+1}(y)$ is easy to compute using the decision policies that the backward-recursion algorithm yields.

Then, we can define the probability distribution, $\xi_t(y)$, of the hour-t SOE of energy storage recursively as:

$$\xi_1(y) = \begin{cases} 1; & \text{if } y = \bar{l}_1; \\ 0; & \text{otherwise;} \end{cases}$$

and:

$$\xi_{t+1}(y) = \sum_{(\lambda,w)\in\mathcal{I}_{t+1}(y)} \text{Prob}\{\omega_t = w\}\,\xi_t(\lambda); \quad \forall t = 1,\ldots,T-1. \quad (10)$$

The Prob$\{\cdot\}$ in (10) is given by the LOLPs, $\{p_t\}_{t=1}^T$.

The intuition behind (10) is that for the hour-$(t+1)$ SOE of energy storage to equal a particular value, y, the hour-t system state must belong to an element of $\mathcal{I}_{t+1}(y)$. λ and w are placeholders for different elements of $\mathcal{I}_{t+1}(y)$. $\xi_t(\lambda)$ gives the probability that the hour-t SOE of energy storage is λ and p_t gives the probability of ω_t being equal to w. Thus, the sum, over all elements of $\mathcal{I}_{t+1}(y)$, of the product of these two probabilities gives the probability with which $l_{t+1} = y$.

D. Computing ELCC of Energy Storage

Combining δ^* with $\{\xi_t(y)\}_{t=1}^T$, we compute the LOLE of the system with the energy storage and $\bar{M}$ MW of load added as:

$$e^{\bar{M}} = \sum_{t=1}^{T}\sum_{y}\xi_t(y)\times$$

$$\text{Prob}\left\{G_t + \eta d_t^{\delta^*}(y,0) < M_t + \bar{M}\right\}; \quad (11)$$

where the Prob$\{\cdot\}$ represents the same sources of uncertainty as in (1). The $\eta d_t^{\delta^*}(y,0)$ term in computing $e^{\bar{M}}$ represents the amount that energy storage contributes toward meeting load during hour t if the system experiences a loss-of-load event, which is why we substitute $\omega_t = 0$ in $d_t^{\delta^*}(y,0)$, and its hour-t SOE is y, which occurs with probability, $\xi_t(y)$.

By definition, the ELCC of energy storage is the value of $\bar{M}$ for which $e = e^{\bar{M}}$.

III. Example

We demonstrate our proposed methodology using a day-long example with random loads, a renewable generator with random production, and five conventional generators. The conventional generators are modeled using random binary states, meaning that each unit is either online, in which case it can produce up to its nameplate capacity, or it is offline, in which case it supplies nothing. All of the random variables (*e.g.*, loads, renewable output, and conventional-generator states) are serially and cross-sectionally independent. Table I summarizes the nameplate capacities and EFORs of the five conventional generators. Fig. 1 shows load, renewable-availability, and energy-price data. During each hour there are two equiprobable scenarios with different loads and two equiprobable scenarios with different renewable-availability levels. These scenarios give four possible net-load levels (*e.g.*, load less renewable availability), each with probability $1/4$.

TABLE I
Nameplate Capacities and EFORs of Conventional Generators in Example from Section III

	Generator				
	1	2	3	4	5
Nameplate Capacity (MW)	75	100	150	150	175
EFOR	0.95	0.95	0.90	0.90	0.93

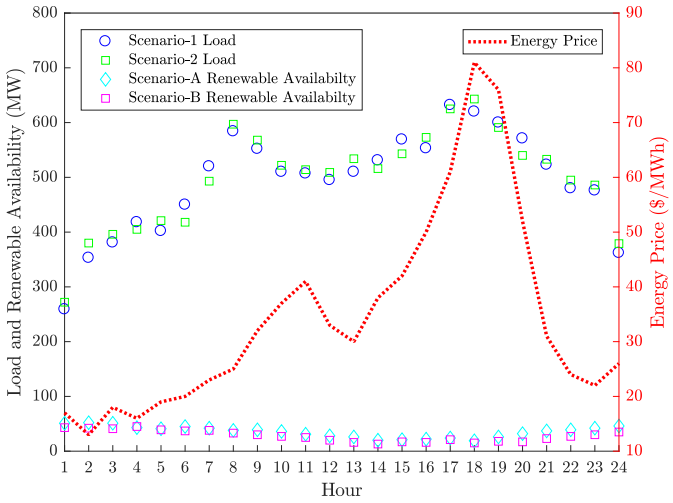

Fig. 1. Loads, renewable availabilites, and energy prices in Example from Section III.

Fig. 2 summarizes the operation of energy storage in the example, assuming that $\bar{h} = 4$, $\bar{R} = 100$, $\eta = 0.75$, $\bar{l}_1 = 100$, $\bar{V} = 1000$, and that no loss-of-load events occur during the day. Despite loss-of-load events not occurring, we observe the non-trivial probabilities of loss-of-load events (which are given by the LOLPs in the lower pane of Fig. 2) and the non-performance penalty (*i.e.*, the nonzero value of $\bar{V}$) impacting energy-storage operations. As expected, energy-storage charging and discharging follow energy-price patterns—energy is charged during the morning when prices are relatively low and discharged later in the day when prices are higher [25].

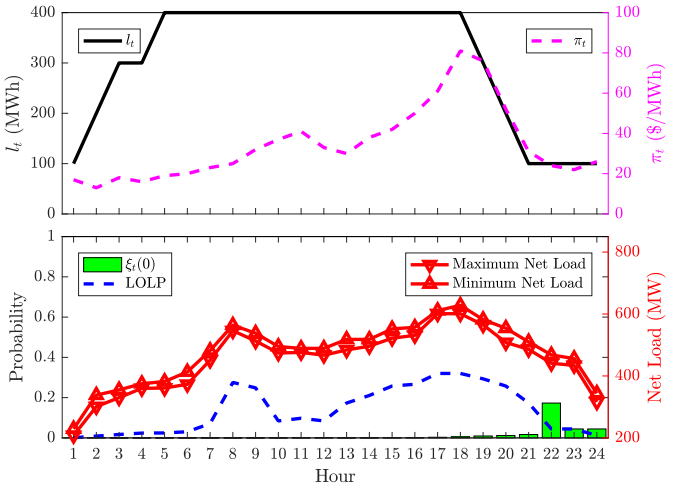

Fig. 2. SOE of energy storage (assuming no loss-of-load events), energy prices, LOLPs, net-load ranges, and $\xi_t(0)$ in Example from Section III with $\bar{h} = 4$ and $\bar{V} = 1000$.

However, the energy storage foregoes some energy-related revenue to maintain a higher SOE to hedge against non-performance penalties should a loss-of-load event occur. Specifically, energy storage is discharged during hours 18–20, when energy prices range between \$52/MWh and \$81/MWh, and during hour 24, when the energy price is \$26/MWh. Importantly, energy storage does not discharge during hour 17, when the energy price is \$61/MWh. Discharging during hour 17, as opposed to during hour 24, would (accounting for $\eta = 0.75$) yield added revenue of \$26.25. This energy revenue is foregone because the power system has relatively high LOLPs throughout hours 17–23. To illustrate the impact of discharging during hour 17, we compute:

$$\sum_{t=18}^{24} \xi_t(0) p_t;$$

which gives the LOLP-weighted probability that energy storage is unable to mitigate a loss-of-load event during hours 18–24. If energy storage is not discharged during hour 17, this probability is 0.0206 as opposed to 0.0225 if its discharged during hour 17.

Fig. 2 shows that $\xi_t(0)$ is not necessarily monotone in time—$\xi_{22}(0) = 0.173$ and $\xi_{21}(0) = 0.017$. We have $\xi_{22}(0) > \xi_{21}(0)$ in this case because the hour-21 LOLP is relatively high and $l_{21} = 100$. If the system experiences an hour-21 loss-of-load event, energy storage would discharge to reduce load curtailment, which would yield $l_{22} = 0$. The hour-22 LOLP is relatively low (compared to the hour-21 LOLP), which is why $\xi_{23}(0) < \xi_{22}(0)$.

Table II summarizes the estimated ELCCs of energy storage in the example with different values of $\bar{h}$ and $\bar{V}$. The ELCCs are normalized by the nameplate net discharging capacity of the energy storage [5], [26], which is 75 MW, because we assume $\bar{R} = 100$ and $\eta = 0.75$ (*cf.* Sections II-B4 and II-B6 regarding the treatment of energy losses). The table shows that increasing either of $\bar{h}$ or $\bar{V}$ can increase the ELCC, although through different effects, which are explored in greater detail in Section V. Increasing $\bar{h}$ gives energy storage greater energy-carrying capacity, meaning that, *ceteris paribus*, energy storage tends to have more energy available to mitigate loss-of-load events. Increasing $\bar{V}$ tends to make energy-storage operations more conservative, in the sense that the SOE is kept higher. This is because a higher value of $\bar{V}$ imposes a larger potential non-performance penalty on energy storage that is unable to mitigate a loss-of-load event.

TABLE II
ELCC OF ENERGY STORAGE (% OF NAMEPLATE NET DISCHARGING CAPACITY) IN EXAMPLE FROM SECTION III

	$\bar{V}$			
$\bar{h}$	0	1000	5000	9000
1	6	71	71	71
2	8	91	92	92
4	20	99	100	100
6	30	100	100	100
8	36	100	100	100

IV. CASE-STUDY DATA

Section V summarizes the results of applying our proposed methodology to two case studies, which are based on data that are obtained from operators of two different systems with different generation mixes—one summer- and the other winter-peaking. Due to data confidentiality, we do not reveal the systems or provide detailed case-study data. Rather, we give a high-level description of the system data that we obtain from the operators and how the data are used to construct our case studies. Each system operator provides us with three historical data sets: generator data, loads, and wholesale energy prices.

Data for each generating unit include generation technology, nameplate capacity, historical hourly production level for the case-study year, and historical hourly outage information. We use these data in different ways, depending upon the generating technology of a particular unit. Dispatchable generators (*e.g.*, nuclear or fossil-fueled units) are modeled using their nameplate capacities and effective forced outage rates (EFORs) in the Prob$\{\cdot\}$ functions that appear in (1) and (11). Specifically, each of these units is represented using Bernoulli trials—each unit is unavailable and produces nothing during a given hour with probability equal to its EFOR and is available to operate at its nameplate capacity during the hour with the complementary probability. This is a standard approach to representing dispatchable generators in power-system-reliability modeling. Each unit's availability during

each hour is serially and cross-sectionally independent. EFORs are approximated using historical outage data. The remaining generators (*e.g.*, wind, solar, and small hydroelectric plants) are assumed to produce during each hour according to their historical production levels. This is a standard approach to representing weather variability, which drives the output of such units, in capacity-valuation exercises [27], [28]. Energy storage is represented as outlined in Section II, as its resource-adequacy contribution depends on its operation and resultant SOE.

Load data specify the historical hourly load during the case-study year for each system. The load data indicate also hourly net exports of energy to neighboring regions and deployment of demand-response resources and private-use networks (which, in most cases, reflect load net of distributed on-site generation by customers). We use these historical data, assuming that the demand-response and private-use-network resources are used in our case study as reported in the historical data. System net load is given by subtracting wind and solar production and demand-response deployment from the sum of load, net exports, and private-use-network deployment. We make an additive adjustment to the loads in computing (1) for each system so that the LOLE of the base system is 2.4 hours. This corresponds to the reliability standard that is set by North American Electric Reliability Corporation of one outage day every ten years [29]. These additive load adjustments allow us to compare the capacity value of energy storage between the two systems, without the LOLEs of the base systems confounding the results [30].

Hourly historical wholesale electricity prices are used in (8). We assume in our case studies that $\bar{R} = 100$ and $\eta = 0.75$ and consider cases with $\bar{h} \in \{1, 2, 4, 6, 8\}$ and $\bar{V} \in [0, 9000]$. Thus, we use our real-world case studies to explore the drivers of the ELCCs that are reported in Table II in greater detail.

The case studies, each of which include several hundred generators, are implemented using `MATLAB` version R2018b on a computer with a 1.80-GHz Intel Core i7 processor and 16 GB of memory. Solving the dynamic optimization model takes less than one second of wall-clock time. However, computing the ELCC of the energy storage takes over two hours, due to the iterative nature of the calculation that is required to equate e and $e^{\bar{M}}$.

V. Case-Study Results

A. Energy-Storage Operations

Fig. 3 summarizes the operation of energy storage in the summer-peaking system during 10 August, 2016 assuming $\bar{h} = 1$ and $\bar{V} = 0$. 10 August, 2016 has relatively high loads and non-trivial LOLPs (the LOLPs for the day sum to 0.2, which is nearly a tenth of the year's LOLE). We focus our analysis on this day (as opposed to a day with extremely high energy-price differences), because LOLPs have a more important impact on the operation of energy storage than energy prices do. The upper pane of Fig. 3 shows that energy prices during the day peak during hour 15. As such, without a financial incentive to keep energy stored to mitigate potential loss of load between hours 16 and 18, energy storage is discharged fully during hour 15 to exploit the high energy prices (the SOEs that are shown in all of Figs. 3–9 assume $\omega_t = 1$ during all hours). As such, the energy storage contributes to system reliability during hours 14 and 15 only and, importantly, not during hour 16, which has the day's highest LOLP.

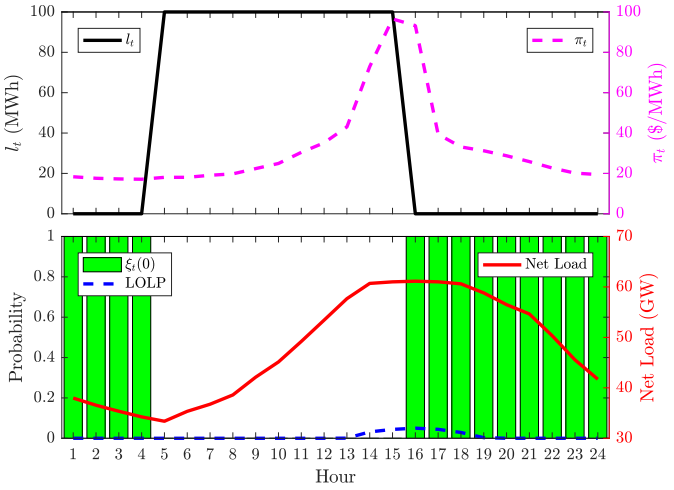

Fig. 3. SOE of energy storage (assuming no loss-of-load events), energy prices, LOLPs, net loads, and $\xi_t(0)$ in summer-peaking case study from Section V during 10 August, 2016 with $\bar{h} = 1$ and $\bar{V} = 0$.

Fig. 4 summarizes the operation of the energy storage in the same setting as in Fig. 3, except that $\bar{V} = 9000$ in the case that is summarized in Fig. 4. Fig. 4 shows that the penalty on not having energy available to discharge during a potential loss-of-load event provides a strong financial incentive to maintain a higher SOE during hours 16–19. The SOE profile that is shown in Fig. 4 assumes $\omega_t = 1$ during all of the hours of the day. Nevertheless, the high LOLPs during hours 16–19 and the nonzero value of $\bar{V}$ impose a high expected cost if the energy storage has a zero SOE during this window of time, which drives the change in the operating pattern between Figs. 3 and 4. Although the LOLPs between hours 20 and 24 are nonzero, they are sufficiently close to zero that the revenue that is earned from discharging stored energy during hour 19 outweighs the expected cost of any non-performance penalties between hours 20 and 24. Although $l_{15} = l_{16} = \cdots = l_{19} = 100$ if $\omega_t = 1, \forall t$, $\xi_{15}(0), \xi_{16}(0), \ldots, \xi_{19}(0)$ are trivially nonzero in Fig. 4. These values of $\xi_t(0)$ are nonzero because during each of hours 15–19, there is a non-trivial probability that a loss-of-load event during an earlier hour results in the energy storage discharging, which would give a zero SOE in a subsequent hour. The recursive calculation of $\xi_t(\cdot)$ in (10) takes account of such intertemporal dynamics.

Contrasting the operational profiles that are shown in Figs. 3 and 4 provides insights into the difference between our current work and that on which we build [17]. The earlier work models the operation of energy storage by optimizing energy revenues only and is akin to cases that we model with $\bar{V} = 0$. Cases with $\bar{V} > 0$ allow us to examine how energy storage is operated if it co-optimizes its energy and reliability values.

Fig. 5 summarizes the operation of the energy storage in the same setting as in Fig. 3, with $\bar{h} = 8$ and $\bar{V} = 0$ in

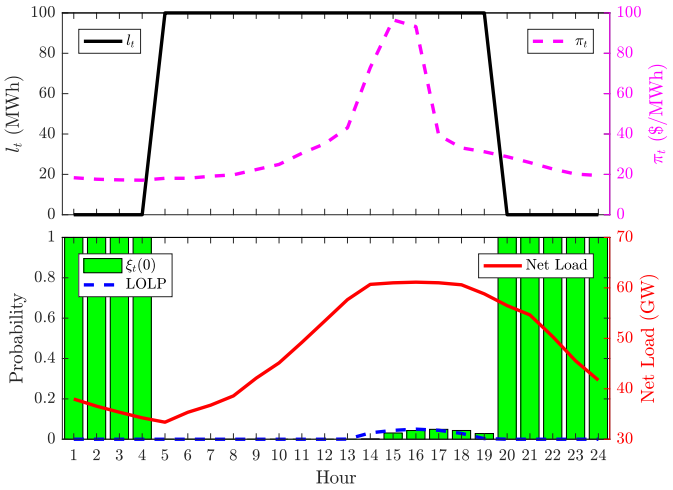

Fig. 4. SOE of energy storage (assuming no loss-of-load events), energy prices, LOLPs, net loads, and $\xi_t(0)$ in summer-peaking case study from Section V during 10 August, 2016 with $\bar{h} = 1$ and $\bar{V} = 9000$.

the case that is summarized in Fig. 5. Fig. 5 shows that with $\bar{h} = 8$ the financial incentive of $\bar{V}$ is not needed for the energy storage to contribute to system reliability during the full window of time between hours 14 and 19 when the system has non-trivial LOLPs. This is due to the relatively high energy-carrying capability of the energy storage with $\bar{h} = 8$. Indeed, the operational profile of energy storage with $\bar{h} = 8$ and $\bar{V} = 9000$, which we exclude for sake of brevity, is exactly the same as that which is shown in Fig. 5.

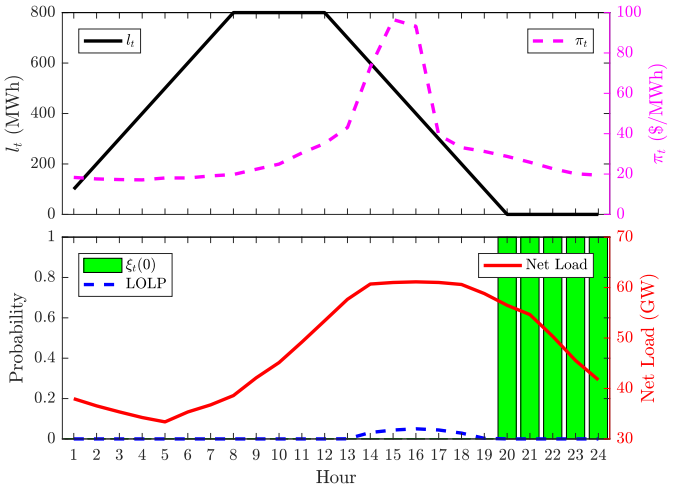

Fig. 5. SOE of energy storage (assuming no loss-of-load events), energy prices, LOLPs, net loads, and $\xi_t(0)$ in summer-peaking case study from Section V during 10 August, 2016 with $\bar{h} = 8$ and $\bar{V} = 0$.

Fig. 6 summarizes the operation of energy storage in the winter-peaking system during 19 January, 2016 assuming $\bar{h} = 1$ and $\bar{V} = 0$. As is common of winter-peaking systems, there are morning and evening load peaks on this day. Prices peak during hour 19, which is coincident with the peak in the LOLPs on this day. However, LOLPs remain non-trivial until hour 21. Because of the relatively high price during hour 19, absent the financial incentive that a non-zero value of $\bar{V}$ provides, the energy storage is discharged and does not contribute to system reliability during hours 20 and 21. Thus, the operational profile that is shown in Fig. 6 exhibits the same myopic behavior with respect to the reliability contribution of energy storage that Fig. 3 shows. Fig. 7 shows that increasing $\bar{V}$ to 9000 has the same qualitative impact on energy-storage operations as that shown in Fig. 4. Namely, the high potential cost of a penalty for not having energy available during a loss-of-load event results in energy storage retaining energy through hour 22, which increases its reliability contribution.

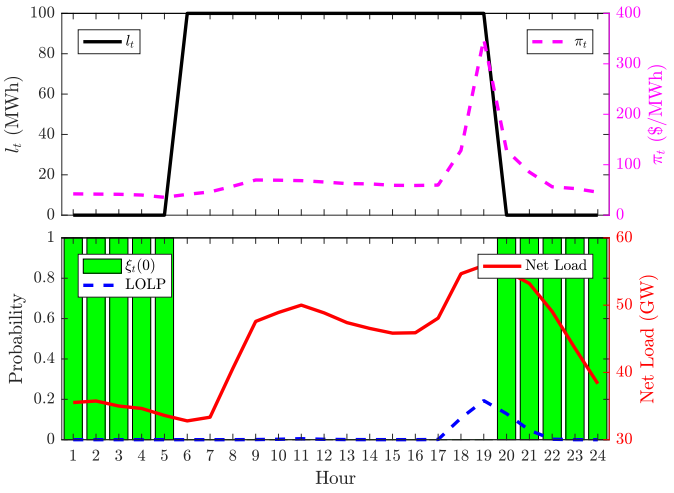

Fig. 6. SOE of energy storage (assuming no loss-of-load events), energy prices, LOLPs, net loads, and $\xi_t(0)$ in winter-peaking case study from Section V during 19 January, 2016 with $\bar{h} = 1$ and $\bar{V} = 0$.

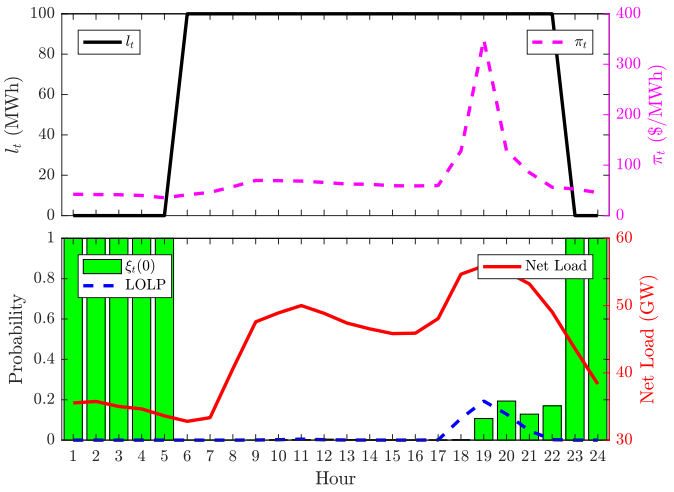

Fig. 7. SOE of energy storage (assuming no loss-of-load events), energy prices, LOLPs, net loads, and $\xi_t(0)$ in winter-peaking case study from Section V during 19 January, 2016 with $\bar{h} = 1$ and $\bar{V} = 9000$.

Fig. 7 shows that energy is retained until hour 22, despite the LOLP being near-zero during that hour. This behavior stems from the hour-22 LOLP being on the order of 10^{-3}, which appears to be near-zero, given the scale of the vertical axis in Fig. 7. Multiplying the scale of the hour-22 LOLP with the value of $\bar{V} = 9000$, means that the expected cost of having no stored energy available during hour 22 is on the order

of \$10[1]. The differences in energy prices between hours 22 and 21 is on the order of \$3.50. These values demonstrate that our model provides operational decisions that tradeoff the monetized energy and reliability values of energy storage.

Figs. 8 and 9 summarize the operation of energy storage with $\bar{h} = 8$ on the same day that is summarized in Figs. 6 and 7, assuming values of $\bar{V} = 0$ and $\bar{V} = 9000$, respectively. As with Fig. 4, we see that the financial incentive that $\bar{V}$ provides to retain stored energy is less crucial if energy storage has sufficient energy-carrying capacity. Nevertheless, having $\bar{V} = 9000$ does result in a small change in the operating profile of the energy storage, which is that energy is retained to contribute to system reliability during hour 22. Fig. 8 shows that absent the financial incentive that $\bar{V}$ provides, the energy storage would discharge its remaining stored energy during hour 21, meaning that it provides no reliability benefit during hour 22.

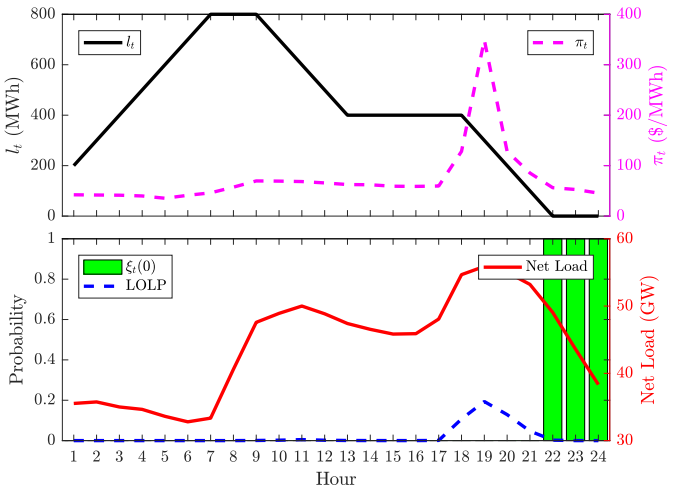

Fig. 8. SOE of energy storage (assuming no loss-of-load events), energy prices, LOLPs, net loads, and $\xi_t(0)$ in winter-peaking case study from Section V during 19 January, 2016 with $\bar{h} = 8$ and $\bar{V} = 0$.

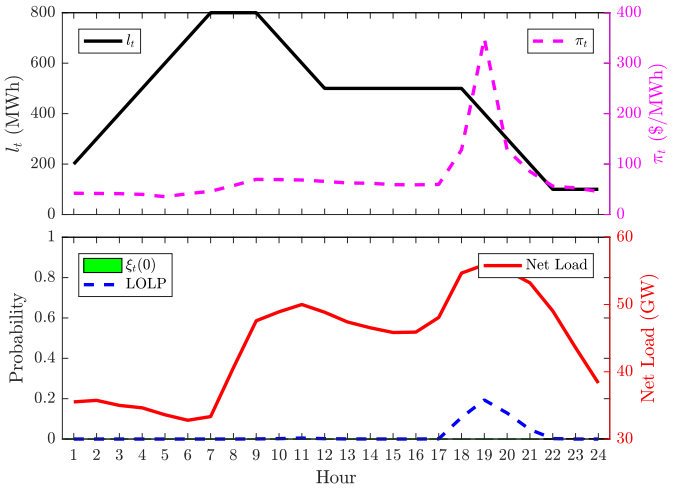

Fig. 9. SOE of energy storage (assuming no loss-of-load events), energy prices, LOLPs, net loads, and $\xi_t(0)$ in winter-peaking case study from Section V during 19 January, 2016 with $\bar{h} = 8$ and $\bar{V} = 9000$.

B. Energy-Storage ELCCs

Tables III and IV summarize the estimated ELCCs of energy storage in the two systems with different values of $\bar{h}$ and $\bar{V}$. The ELCCs are normalized by the 75-MW nameplate net discharging capacity of the energy storage. As shown in Table II and expected from Figs. 3–9, the ELCC is increasing in $\bar{h}$ and $\bar{V}$.

TABLE III
ELCC OF ENERGY STORAGE IN SUMMER-PEAKING CASE STUDY FROM SECTION V (% OF NAMEPLATE NET DISCHARGING CAPACITY)

	$\bar{V}$			
$\bar{h}$	0	1000	5000	9000
1	32	81	91	93
2	60	89	96	99
4	81	97	100	100
6	97	100	100	100
8	100	100	100	100

TABLE IV
ELCC OF ENERGY STORAGE IN WINTER-PEAKING CASE STUDY FROM SECTION V (% OF NAMEPLATE NET DISCHARGING CAPACITY)

	$\bar{V}$			
$\bar{h}$	0	1000	5000	9000
1	41	83	89	92
2	67	95	97	99
4	92	100	100	100
6	95	100	100	100
8	95	100	100	100

The tables show that if there is a strong financial incentive, energy-limited energy storage (*e.g.*, with $\bar{h} = 1$) can have relatively high ELCCs. This result is due to the load patterns. Most systems experience a limited number of consecutive hours of relatively high loads and LOLPs (*cf.* the load and LOLP patterns that are summarized in Figs. 3–9). As such, there is a low likelihood that energy storage (even with $\bar{h} = 1$) is unable to provide energy during a loss-of-load event.

To illustrate this concept concretely, consider the LOLPs on the day that is shown in Figs. 6–9. This day has four hours (18–21) with non-trivial LOLPs, which are summarized in Table V. With a sufficiently high value of $\bar{V}$, energy storage with $\bar{h} = 1$ is operated so it is charged fully as of the beginning of hour 18. As such, $\xi_{18}(0) \approx 0$.[2] Moreover, energy storage has a 0.89 probability of being fully charged as of the beginning of hour 19 (*i.e.*, it would be discharged if there is a loss-of-load event during hour 18, which occurs with probability 0.11). If there is no stored energy available as of the beginning of hour 19, so long as the system does not experience loss of load during hour 19, the energy storage recharges during hour 19, and has energy available during hour 20. Thus, in such a case, energy storage *does* contribute to system reliability during hour 20, even if it has no reliability contribution during hour 19. The recursive calculation of $\xi_t(\cdot)$ in (10), which

[2]There is a minuscule probability that $l_{18} = 0$, which occurs if there is a loss-of-load event during hour 17, which is highly unlikely because $p_{17} \approx 0$.

underlies calculations of the ELCC of energy storage, takes account of these types of intertemporal dynamics.

TABLE V
NON-TRIVIAL LOLPS FOR WINTER-PEAKING CASE STUDY FROM SECTION V DURING 19 JANUARY, 2016

t	18	19	20	21
p_t	0.11	0.19	0.13	0.05

We use three measures of energy-limited energy storage with a relatively low value of $\bar{h}$ benefiting from the low likelihood of numerous consecutive hours with relatively high LOLPs. The first metric is the average (over the year that is modeled) number of consecutive hours during which the LOLP is at least, $\bar{p}$, conditional upon at least one hour having an LOLP greater than or equal to $\bar{p}$. Put another way, if $p_t \geq \bar{p}$ for some $t = 1, \ldots, T$, this first metric determines how many subsequent consecutive hours have LOLPs of at least $\bar{p}$. The second metric is the number of days of the year with two or more hours with LOLPs of at least $\bar{p}$. The third metric is:

$$\sum_{t \in T} \xi_t(0) p_t \mathbf{1}_{\{p_t \geq \bar{p}\}}; \tag{12}$$

where $\mathbf{1}_{\{p_t \geq \bar{p}\}}$ is the indicator that $p_t \geq \bar{p}$. Equation (12) computes an LOLP-weighted average probability that the energy storage is depleted (and unable to supply energy) during periods with LOLPs of at least $\bar{p}$.

Table VI summarizes the values of these three metrics for the two systems for energy storage with $\bar{h} = 1$ and assuming $\bar{p} = 0.01$. The table shows that, on average, there are relatively short blocks of time with high LOLPs. The summer-peaking system has, on average, four-hour blocks of consecutive hours with LOLPs above 0.01 as opposed to an average of two-hour blocks for the winter-peaking system. This difference in the average duration of the blocks explains the lower ELCCs for energy storage in the summer-peaking system for all values of $\bar{h}$ and $\bar{V}$ relative to the ELCCs for the winter-peaking system (*cf.* Tables III and IV).

TABLE VI
ELCC-RELATED METRICS FOR ENERGY STORAGE FOR CASE STUDY FROM SECTION V WITH $\bar{h} = 1$ ($\bar{p} = 0.01$)

	System	
Metric	Summer-Peaking	Winter-Peaking
Average Consecutive Hours With $p_t \geq \bar{p}$	3.91	1.96
Number of Days With $p_t \geq \bar{p}$	11	14
$\sum_{t \in T} \xi_t(0) p_t \mathbf{1}_{\{p_t \geq \bar{p}\}}$	0.015	0.004

C. Energy-Storage Profits

Tables VII and VIII summarize the expected energy profits that energy storage earns in the two systems for different values of $\bar{h}$ and $\bar{V}$. The profits that are reported do not account for expected non-performance penalties. Profit is increasing in $\bar{h}$, which reflects the incremental value of increasing the energy-carrying capability of energy storage [25]. Increasing the capacity of energy storage allows it to arbitrage prices differences between more pairs of hours. However, marginal profits are diminishing, because the price differences between the hours that are arbitraged with additional energy-carrying capacity are smaller.

TABLE VII
ANNUAL EXPECTED ENERGY PROFIT FOR ENERGY STORAGE IN SUMMER-PEAKING CASE STUDY FROM SECTION V ($ MILLION)

	$\bar{V}$			
$\bar{h}$	0	1000	5000	9000
1	0.809	0.755	0.658	0.590
2	1.426	1.393	1.346	1.324
4	2.132	2.124	2.111	2.104
6	2.489	2.487	2.486	2.485
8	2.652	2.652	2.652	2.651

TABLE VIII
ANNUAL EXPECTED ENERGY PROFIT FOR ENERGY STORAGE IN WINTER-PEAKING CASE STUDY FROM SECTION V ($ MILLION)

	$\bar{V}$			
$\bar{h}$	0	1000	5000	9000
1	2.571	2.494	2.353	2.249
2	3.910	3.886	3.848	3.825
4	4.967	4.966	4.962	4.959
6	5.275	5.275	5.273	5.272
8	5.401	5.401	5.400	5.400

Profit is decreasing in $\bar{V}$, which reflects two effects of $\bar{V}$ on energy-storage operations. The first is that energy storage may not discharge stored energy during the highest-priced hours, as illustrated in Figs. 3 and 4. Fig. 3 shows that with $\bar{V} = 0$, stored energy is discharged during hour 15, when the price peaks for the day at $96.56/MWh. Taking into account $\eta = 0.75$ and the $17.11/MWh price of charging energy, means that the energy storage earns $55.31 during the day. With $\bar{V} = 9000$, Fig. 4 shows that the stored energy is discharged during hour 19 after the high-LOLP period when the energy price is $31.21. This operating profile yields a net profit to the energy storage of $6.30/MW for the day.

Another profit impact that $\bar{V}$ has, which is illustrated in Figs. 8 and 9, is that with $\bar{V}$ sufficiently high, some stored energy may not be discharged. Fig. 8 shows that with $\bar{V} = 0$, the last incremental hour of energy-carrying capacity is discharged during hour 21, when the energy price is $85.38/MWh. Taking account of the $41.23/MWh cost of the last increment of charging energy, this yields the energy storage a net profit of $22.81/MW from this last increment of energy-carrying capacity. With $\bar{V} = 9000$, the last increment of stored energy is retained until the end of the high-LOLP period in hour 22, when the energy price is $56.23/MWh. Thus, discharging this last increment of energy during hour 22 would yield a net profit of $0.94/MW. Given that energy must be stored for high LOLPs during the subsequent day, it is more economic to retain this last increment of stored energy.

Taken together, these profit impacts of $\bar{V}$ imply that energy storage must be remunerated for operating in a manner to co-optimize its energy and reliability benefits. The design of such a remuneration mechanism is beyond the scope of our work. Rather, our inclusion of $\bar{V}$ in (8) could reflect, as an example, non-performance penalties that are imposed on resources that participate in organized capacity mechanisms (*e.g.*, PJM Interconnection's Reliability Pricing Model or ISO New England's Forward Capacity Market).

VI. Conclusions

This paper expands upon previous work [17] to develop a stochastic operational model that co-optimizes energy and reliability benefits of energy storage. Our model abstracts the details of how reliability benefits are monetized. We assume that energy storage is remunerated for its reliability benefits but that financial penalties (*e.g.*, $\bar{V}$) are imposed for real-time non-performance. Setting $\bar{V} = 0$ provides operational strategies that maximize energy value to the exclusion of reliability benefit. An example and two comprehensive case studies are used to demonstrate the operation, ELCC, and operating profit of energy storage, including the impacts of $\bar{h}$ and $\bar{V}$ thereon.

Our example includes generator failure and random load and renewable-energy production as sources of uncertainty. Our case study focuses on generator failures as sources of uncertainty. Our model could be applied easily to a case with serial correlation (*e.g.*, modeling Markovian generator failures). Serial correlations would impact the state-transition probabilities that determine the values of ω_t during each stage.

In addition to providing decision support for an energy-storage operator, our model can help guide current market-design and policy decisions. Market operators are updating their tariffs to allow energy storage to participate in their systems as capacity resources. Much of this market development is in reaction to Federal Energy Regulatory Commission order 841.[3] Some markets are proposing *ad hoc* rules with respect to treating energy storage as capacity resources. For instance, California's Resource Adequacy construct requires four hours of energy-carrying capability for energy storage to be treated as having a 100% capacity rating. Other market operators are proposing requiring energy-carrying capabilities of eight or more hours. Our results show that depending upon the load patterns, without a financial penalty, eight hours of energy-carrying capability may yield an ELCC below 100% (*cf.* Table IV). On the other hand, if there are sufficient financial incentives, energy storage with two hours of energy-carrying capability may have a near-100% capacity rating. Intuitively, a nonzero value of $\bar{V}$ is needed because energy prices may peak before LOLPs (*cf.* Fig. 3) or because, even if price and LOLP peaks are co-incident, energy storage that is focused on energy revenue only may discharge before it should from the perspective of reliability benefit (*cf.* Fig. 6).

[3] *cf.* docket number RM16-23-000 for filings and decisions.

Acknowledgment

The authors thank A. Sorooshian, A. J. Conejo, the editors, and four anonymous reviewers for suggestions and comments.

References

[1] R. Sioshansi, P. Denholm, and T. Jenkin, "Market and Policy Barriers to Deployment of Energy Storage," *Economics of Energy & Environmental Policy*, vol. 1, pp. 47–63, March 2012.

[2] X. Xi, R. Sioshansi, and V. Marano, "A Stochastic Dynamic Programming Model for Co-optimization of Distributed Energy Storage," *Energy Systems*, vol. 5, pp. 475–505, September 2014.

[3] X. Xi and R. Sioshansi, "A Dynamic Programming Model of Energy Storage and Transformer Deployments to Relieve Distribution Constraints," *Computational Management Science*, vol. 13, pp. 119–146, January 2016.

[4] A. Tuohy and M. O'Malley, "Impact of Pumped Storage on Power Systems with Increasing Wind Penetration," in *2009 IEEE Power & Energy Society General Meeting*. Calgary, Alberta, Canada: Institute of Electrical and Electronics Engineers, 26-30 July 2009, pp. 1–8.

[5] S. H. Madaeni, R. Sioshansi, and P. Denholm, "Estimating the Capacity Value of Concentrating Solar Power Plants with Thermal Energy Storage: A Case Study of the Southwestern United States," *IEEE Transactions on Power Systems*, vol. 28, pp. 1205–1215, May 2013.

[6] R. Perez, M. Taylor, T. Hoff, and J. P. Ross, "Reaching Consensus in the Definition of Photovoltaics Capacity Credit in the USA: A Practical Application of Satellite-Derived Solar Resource Data," *IEEE Journal of Selected Topics in Applied Earth Observations and Remote Sensing*, vol. 1, pp. 28–33, March 2008.

[7] R. Billinton and P. Wang, "Distribution System Reliability Cost/Worth Analysis Using Analytical and Sequential Simulation Techniques," *IEEE Transactions on Power Systems*, vol. 13, pp. 1245–1250, November 1998.

[8] B. Bagen and R. Billinton, "Impacts of Energy Storage on Power System Reliability Performance," in *2005 Canadian Conference on Electrical and Computer Engineering*. Saskatoon, Saskatchewan, Canada: Institute of Electrical and Electronics Engineers, 1-4 May 2005, pp. 494–497.

[9] P. Hu, R. Karki, and R. Billinton, "Reliability evaluation of generating systems containing wind power and energy storage," *IET Generation, Transmission & Distribution*, vol. 3, pp. 783–791, August 2009.

[10] L. H. Koh, G. Z. Yong, W. Peng, and K. J. Tseng, "Impact of Energy Storage and Variability of PV on Power System Reliability," *Energy Procedia*, vol. 33, pp. 302–310, 2013.

[11] Y. Zhou, P. Mancarella, and J. Mutale, "Framework for capacity credit assessment of electrical energy storage and demand response," *IET Generation, Transmission & Distribution*, vol. 10, pp. 2267–2276, 9 June 2016.

[12] I. Konstantelos, P. Djapic, G. Strbac, P. Papadopoulos, and A. Laguna, "Contribution of energy storage and demand-side response to security of distribution networks," *CIRED - Open Access Proceedings Journal*, vol. 2017, pp. 1650–1654, October 2017.

[13] I. Konstantelos and G. Strbac, "Capacity value of energy storage in distribution networks," *Journal of Energy Storage*, vol. 18, pp. 389–401, August 2018.

[14] R. Billinton and R. N. Allan, *Reliability Evaluation of Power Systems*. Boston, Massachusetts: Pitman Advanced Publishing Program, 1984.

[15] B. Klöckl and G. Papaefthymiou, "An effort to overcome the chronological modeling methods for energy storage devices," in *2005 International Conference on Future Power Systems*. Amsterdam, Netherlands: Institute of Electrical and Electronics Engineers, 18 November 2005.

[16] G. Edwards, S. Sheehy, C. J. Dent, and M. C. M. Troffaes, "Assessing the contribution of nightly rechargeable grid-scale storage to generation capacity adequacy," *Sustainable Energy, Grids and Networks*, vol. 12, pp. 69–81, December 2017.

[17] R. Sioshansi, S. H. Madaeni, and P. Denholm, "A Dynamic Programming Approach to Estimate the Capacity Value of Energy Storage," *IEEE Transactions on Power Systems*, vol. 29, pp. 395–403, January 2014.

[18] M. Amelin, "Comparison of Capacity Credit Calculation Methods for Conventional Power Plants and Wind Power," *IEEE Transactions on Power Systems*, vol. 24, pp. 685–691, May 2009.

[19] G. R. Pudaruth and F. Li, "Capacity Credit Evaluation: A literature review," in *Third International Conference on Electric Utility Deregulation and Restructuring and Power Technologies*. Nanjing, China: Institute of Electrical and Electronics Engineers, 6-9 April 2008, pp. 2719–2724.

[20] W. B. Powell, *Approximate Dynamic Programming: Solving the Curses of Dimensionality*. Hoboken, New Jersey: Wiley-Interscience, 2007.

[21] R. Sioshansi and A. J. Conejo, *Optimization in Engineering: Models and Algorithms*, ser. Springer Optimization and Its Applications. Gewerbestraße 11, 6330 Cham, Switzerland: Springer Nature, 2017, vol. 120.

[22] J. B. Greenblatt, S. Succar, D. C. Denkenberger, R. H. Williams, and R. H. Socolow, "Baseload wind energy: modeling the competition between gas turbines and compressed air energy storage for supplemental generation," *Energy Policy*, vol. 35, pp. 1474–1492, March 2007.
[23] R. Sioshansi, "Welfare Impacts of Electricity Storage and the Implications of Ownership Structure," *The Energy Journal*, vol. 31, pp. 173–198, 2010.
[24] *PJM Manual 18: PJM Capacity Market*, 47th ed., PJM Interconnection, 27 January 2021.
[25] R. Sioshansi, P. Denholm, T. Jenkin, and J. Weiss, "Estimating the Value of Electricity Storage in PJM: Arbitrage and Some Welfare Effects," *Energy Economics*, vol. 31, pp. 269–277, March 2009.
[26] D. McConnell, T. Forcey, and M. Sandiford, "Estimating the value of electricity storage in an energy-only wholesale market," *Applied Energy*, vol. 159, pp. 422–432, 1 January 2015.
[27] A. Keane, M. R. Milligan, C. J. Dent, B. Hasche, C. D'Annunzio, K. Dragoon, H. Holttinen, N. Samaan, L. Söder, and M. O'Malley, "Capacity Value of Wind Power," *IEEE Transactions on Power Systems*, vol. 26, pp. 564–572, May 2011.
[28] D. Gami, R. Sioshansi, and P. Denholm, "Data Challenges in Estimating the Capacity Value of Solar Photovoltaics," *IEEE Journal of Photovoltaics*, vol. 7, pp. 1065–1073, July 2017.
[29] E. P. Kahn, "Effective Load Carrying Capability of Wind Generation: Initial Results with Public Data," *The Electricity Journal*, vol. 17, pp. 85–95, December 2004.
[30] S. H. Madaeni, R. Sioshansi, and P. Denholm, "Estimating the Capacity Value of Concentrating Solar Power Plants: A Case Study of the Southwestern United States," *IEEE Transactions on Power Systems*, vol. 27, pp. 1116–1124, May 2012.

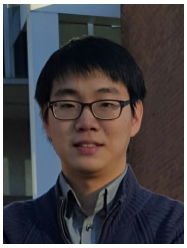

Hyeong Jun Kim (S'16) received his B.S. degree in industrial and management engineering from Hanyang University, South Korea, and an M.S. in industrial and systems engineering from The Ohio State University, Columbus, OH, USA. Currently, he is pursuing a Ph.D. degree at the Ohio State University.

His research interests are in optimization, energy storage, energy-market analysis, and game theory.

Ramteen Sioshansi (M'11–SM'12–F'21) holds the B.A. degree in economics and applied mathematics and the M.S. and Ph.D. degrees in industrial engineering and operations research from University of California, Berkeley, Berkeley, CA, USA and an M.Sc. in econometrics and mathematical economics from London School of Economics and Political Science, London, U.K.

He is a professor in Department of Integrated Systems Engineering and Department of Electrical and Computer Engineering at The Ohio State University, Columbus, OH, USA. His research focuses on the analysis of renewable and sustainable energy systems and the design of restructured competitive electricity markets.

Eamonn Lannoye (M'09) received B.E. and Ph.D. degrees from University College Dublin, Dublin, Ireland and an MBA from Imperial College London, London, U.K.

He works as Senior Project Manager at EPRI Europe where his interests include grid reliability, transmission-system operation, and the interface between transmission-system and distribution-system operators.

Erik Ela (M'06–SM'15) received the B.S.E.E. degree from Binghamton University, Binghamton, NY, USA, the M.S. degree from Illinois Institute of Technology, Chicago, IL, USA, and the Ph.D. degree from University College Dublin, Dublin, Ireland.

He is currently a Principal Technical Leader at Electric Power Research Institute. He has held positions at National Renewable Energy Laboratory and New York Independent System Operator. His research interests include power-system operations, electricity-market design, power-system planning, and reliability services.